Mechanism of cGMP-gated Channel Block by Intracellular Polyamines

Donglin Guo and Zhe Lu

From the Department of Physiology, University of Pennsylvania, Philadelphia, Pennsylvania 19104

abstract Polyamines block the retinal cyclic nucleotide-gated channel from both the intracellular and extracellular sides. The voltage-dependent mechanism by which intracellular polyamines inhibit the channel current is complex: as membrane voltage is increased in the presence of polyamines, current inhibition is not monotonic, but exhibits a pronounced damped undulation. To understand the blocking mechanism of intracellular polyamines, we systematically studied the endogenous polyamines as well as a series of derivatives. The complex channel-blocking behavior of polyamines can be accounted for by a minimal model whereby a given polyamine species (e.g., spermine) causes multiple blocked channel states. Each blocked state represents a channel occupied by a polyamine molecule with characteristic affinity and probability of traversing the pore, and exhibits a characteristic dependence on membrane voltage and cGMP concentration.

key words: retinal cyclic guanine monophosphate–gated channel • ion permeation • protonation • polyamine • diamine

INTRODUCTION

Cyclic nucleotide–gated (CNG)[1] channels are a class of nonselective cation channels present in many tissue types. CNG channels open when cAMP and/or cGMP binds to a cyclic nucleotide–binding motif formed by part of the COOH-terminal segment of the channel polypeptide chain (Kaupp et al., 1989; Goulding et al., 1994; Varnum et al., 1995; Sunderman and Zagotta, 1999). Since the channel is almost equally permeable to Na$^+$ and K$^+$, the current through the channel reverses near zero membrane potential under physiological ionic conditions (Werblin, 1975; Bader et al., 1979; Yau et al., 1981; Bastian and Fein, 1982; Woodruff et al., 1982; Capovilla et al., 1983; Hodgkin et al., 1984, 1985; Yau and Nakatini, 1984; Bododia and Detwiler, 1985; Baylor and Nunn, 1986). Consequently, opening of the CNG channel depolarizes the cell membrane, whereas closure hyperpolarizes the membrane. In mammalian rod-type photoreceptors, the CNG channel mediates visual signal transduction by opening or closing in response to the binding or unbinding of intracellular cGMP, whose concentration is elevated in darkness and lowered by light. The CNG channel in rods normally is largely blocked by cations. Block of the channel dramatically reduces the contribution of time-averaged current through individual channels to the overall changes in membrane potential. Consequently, the noise of membrane potential in rods is very low, permitting them to detect a change in the level of illumination with extraordinarily high sensitivity (Yau and Baylor, 1989).

For more than a decade, the CNG channel has been known to be blocked by divalent cations such as Ca^{2+} and Mg^{2+} (Haynes et al., 1986; Stern et al., 1987; Colamartino et al., 1991; Zimmerman and Baylor, 1992; Root and MacKinnon, 1993; Eismann et al., 1994; Park and MacKinnon, 1995). Both Ca^{2+} and Mg^{2+} are permeant blockers: they traverse the channel but at a much slower rate than Na$^+$ and K$^+$ ions (Capovilla et al., 1983; Hodgkin et al., 1985; Torre et al., 1987; Nakatani and Yau, 1988). Recently, the channel was also shown to be blocked by the polycationic polyamines putrescine, spermidine, and spermine, from both the extracellular and intracellular sides of the membrane (Lu and Ding, 1999). Thus far, four types of ion channel (inward-rectifier K$^+$, glutamate-gated, acetylcholine (ACh)-receptor, and CNG channels) have been shown to be blocked by (intracellular and/or extracellular) polyamines. The following picture emerges: a channel that can be blocked by Ca^{2+} and Mg^{2+} is also blocked by polyamines (Ault et al., 1980; Mayer et al., 1984; Nowak et al., 1984; Horie et al., 1987; Matsuda et al., 1987; Vandenberg, 1987; Mathie et al., 1990; Ifune and Steinback, 1991; Sands and Barish, 1992; Araneda et al., 1993; Benveniste and Mayer, 1993; Ficker et al., 1994; Lopatin et al., 1994; Bowie and Mayer, 1995; Donevan and Rogawski, 1995; Fakler et al., 1995; Isa et al., 1995; Kamboj et al., 1995; Koh et al., 1995; Igarashi and Williams, 1995; Rock and Macdonald, 1992a,b; Bähring et al., 1997; Chao et al., 1997; Williams, 1997; Bowie et al., 1998; Cu et al., 1998; Haghighi and Cooper, 1998; Lu and Ding, 1999). Polyamines block glutamate-gated channels and ACh-receptor channels in a per-

Address correspondence to Dr. Zhe Lu, University of Pennsylvania, Department of Physiology, D302A Richard Building, 3700 Hamilton Walk, Philadelphia, PA 19104. Fax: 215-573-1940; E-mail: zhelu@mail.med.upenn.edu

[1]*Abbreviations used in this paper:* ACh, acetylcholine; CNG channel, cyclic nucleotide–gated channel; PhTx, philanthotoxin-343.

meant manner. Although polyamines were not previously viewed as permeant blockers for the inward-rectifier K^+ channels, they may also traverse that channel, but to a much lesser extent (Guo and Lu, 2000).

Extracellular polyamine block of CNG channels is very similar to intracellular polyamine block of glutamate-gated and ACh-receptor channels (e.g., compare Bähring et al., 1997, and Haghighi and Cooper, 1998, with Lu and Ding, 1999). That is, the extent of channel block is a bell-shaped function of membrane voltage, which is the hallmark of a permeant ionic pore blocker. In contrast, intracellular polyamine block of CNG channels is much more complex (Lu and Ding, 1999). In the present study, we examine the mechanism of intracellular polyamine block of the CNG channel.

METHODS

Molecular Biology and Oocyte Preparation

The cDNA of the bovine rod cGMP-gated channel α subunit cloned into pGEM-HE plasmid was kindly provided by Dr. Steven A. Siegelbaum (Kaupp et al., 1989; Liman et al., 1992; Goulding et al., 1992, 1993), and the E363G mutant cDNA clone was kindly provided by Dr. Roderick MacKinnon (Root and MacKinnon, 1993). RNA was synthesized using T7 polymerase (Promega) from Nhe1-linearized cDNA. Oocytes harvested from *Xenopus laevis* (Xenopus One) were incubated in a solution containing (mM): 82.5 NaCl, 2.5 KCl, 1.0 MgCl₂, 5.0 HEPES, pH 7.6, and 2–4 mg/ml collagenase. The oocyte preparation was agitated using a platform shaker (80 rpm) for 60–90 min. It was then rinsed thoroughly with and stored in a solution containing (mM): 96 NaCl, 2.5 KCl, 1.8 CaCl₂, 1.0 MgCl₂, 5 HEPES, pH 7.6, and 50 μg/ml gentamicin. Defolliculated oocytes were selected and injected with RNA at least 2 and 16 h, respectively, after collagenase treatment. All oocytes were stored in an incubator at 18°C.

Patch Recording and Data Analysis

The CNG channel currents were recorded in the inside-out configuration from the membrane of *Xenopus* oocytes (injected with the CNG channel cRNA) with an Axopatch 200B amplifier (Axon Instruments, Inc.). The recorded signal was filtered at 1 kHz and sampled at 5 kHz using an analogue-to-digital converter (DigiData 1200; Axon Instruments, Inc.) interfaced with a personal computer. pClamp6 software (Axon Instruments, Inc.) was used to control the amplifier and acquire the data. Macroscopic current–voltage curves were recorded as membrane voltage was linearly ramped (25 mV/s). The currents obtained in the absence of cGMP were used as templates for subsequent off-line background current corrections. All curve fittings were carried out using Origin software version 5 (Microcal Software, Inc.).

Recording Solutions

Both the intracellular and extracellular solutions contained (mM) 130 NaCl, 0.5 EDTA, and 10 HEPES, pH 7.6 or 8.6, as specified. Unless specified otherwise, to activate the channel, 1 mM cGMP was included in the intracellular solution. The intracellular solutions containing diamines, polyamines, and philanthotoxin-343 (PhTx) were prepared daily.

Effect of a Pore Mutation on CNG Channel Block by Spermine

Fig. 1 A shows the macroscopic current–voltage relationship of the wild-type retinal CNG channel in the absence and presence of various concentrations of intracellular spermine. The data were recorded in the inside-out configuration by ramping the membrane voltage from −80 to +80 mV. In the absence of blocking ions, the I-V curve is nearly linear. Spermine in the intracellular solution inhibits the current in a voltage-dependent manner.

Fig. 1 B shows the I-V curves of the E363G mutant channel in the absence and presence of various concentrations of spermine. As previously reported, glycine substitution for residue E363 dramatically reduces the inward current (Root and MacKinnon, 1993; Eismann et al., 1994). Besides its effect on monovalent cation conduction, residue E363 forms the binding site for extracellular divalent cations and also influences channel block by intracellular divalent cations (Root and MacKinnon, 1993; Eismann et al., 1994; Park and MacKinnon, 1995). Furthermore, protonation of a glutamate residue (pKa = 7.6) in the olfactory CNG channel, equivalent to E363 in the retinal CNG channel, reduces the single-channel current by producing subconductance states (Root and MacKinnon, 1994; see also Goulding et al., 1992). As shown in Fig. 1 B, inhibition of the E363G mutant channel by intracellular spermine, like that of the wild-type channel, depends on membrane voltage.

Fig. 1, C and D, shows the fractions of unblocked wild-type and mutant CNG currents as a function of voltage, in the presence of various concentrations of spermine. Wild-type channel block by intracellular polyamine varies with membrane voltage in a complex manner: it increases when the membrane voltage is increased from −80 to −20 mV, and then decreases as the voltage approaches +25 mV, and increases again when the voltage is further increased. Consequently, the blocking curves shown in Fig. 1 C display a minimum followed by a maximum. Fig. 1 D shows that E363G mutation merely shifts the spermine-blocking curves by approximately +40 mV without altering their general multiphasic appearance, as if residue E363 (located at the external end of the ion conduction pore) affects spermine block by a through-space electrostatic effect. This observation supports the idea that intracellular spermine inhibits the CNG channel by acting as a pore blocker.

Comparison of CNG Channel Block by Intracellular Spermine and Putrescine

Fig. 2, A and C, compares the effects of spermine and putrescine on the I-V curve of the wild-type CNG channel. Fig. 2, B and D, plots the corresponding fractions
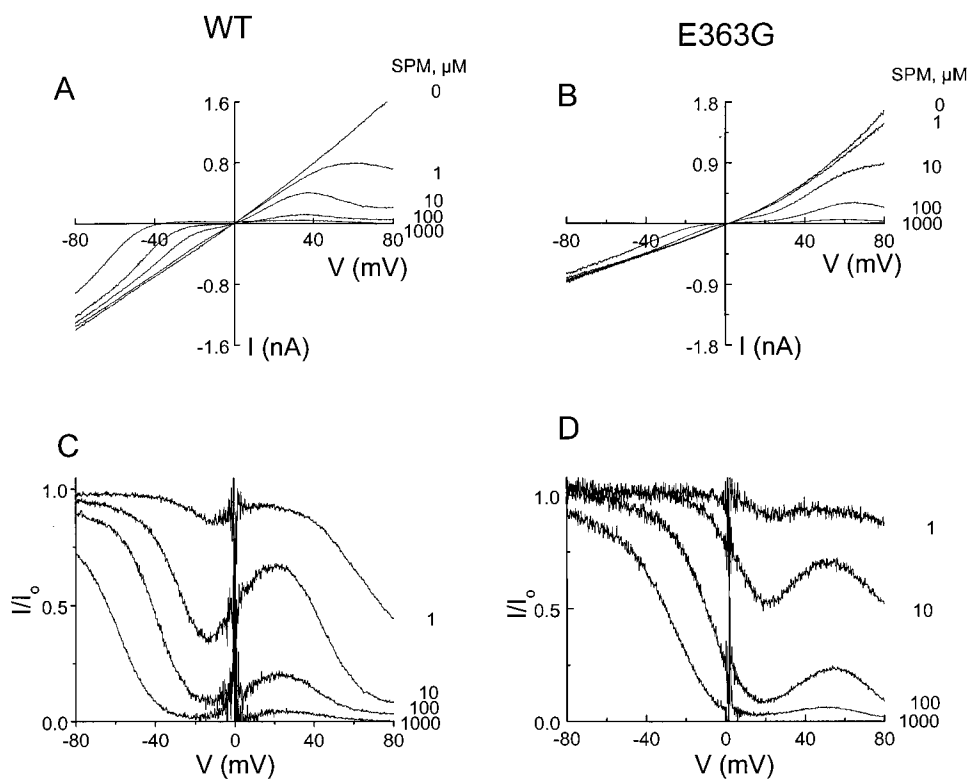
WT

E363G

Figure 1. Effects of mutation at E363 on CNG channel block by spermine. (A and B) Macroscopic I-V curves of wild-type and mutant E363G channels, respectively, in the absence and presence of various concentrations of intracellular spermine. (C and D) The fractions of unblocked currents of wild-type and mutant channels in the presence of various concentrations of spermine are plotted as a function of membrane voltage.

of unblocked current as a function of membrane voltage between −80 and +80 mV. As discussed above, the spermine-blocking curve in Fig. 2 B has a minimum followed by a maximum. In contrast, the putrescine-blocking curve has only a minimum, although it appears to reach a plateau at +80 mV (Fig. 2 D; Lu and Ding, 1999). This difference may result from fundamental differences in the structure of the blockers or merely reflect the fact that putrescine has only two rather than four amine groups. In the latter case, putrescine should exhibit a spermine-like behavior if the membrane voltage range were extended twofold to compensate for the twofold difference in charged groups between putrescine and spermine. To test these possibilities, we examined channel block by putrescine over a much wider range of membrane voltage. Fig. 2 E shows the I-V curves of the channel between −160 and +160 mV in the absence and presence of putrescine. Even in the absence of putrescine, the I-V curve exhibited a slight downward curvature above +140 mV, likely resulting from channel block by traces of endogenous (or contaminating) blockers. In Fig. 2 F, we plotted the fraction of unblocked current in the presence of putrescine as a function of membrane voltage. The putrescine-blocking curve between −160 and +160 mV is qualitatively similar (a minimum followed by a maximum) to that of spermine over a narrower voltage range, as if a twofold reduction in the number of amine groups is roughly compensated by a twofold wider voltage range. Still, despite a twofold compensation in

membrane voltage, the putrescine-blocking curve differs somewhat from that of spermine, undoubtedly because of the two additional segments in spermine.

Block of the CNG Channel by a Series of Diamines

To learn how methylene groups affect the blocking behavior of polyamines, we examined CNG channel block by a series of putrescine analogues—diamines with methylene (CH_2) chains of varying length between the two amine groups. To obtain a more complete picture of their blocking behaviors, we further increased the voltage range to between −180 and +180 mV—the widest range within which we could collect sufficient data before the oocyte membrane ruptured. Fig. 3 shows the I-V curves of the CNG channels in the absence and presence of several concentrations of nine diamines, denoted DM_{C2} through DM_{C10}, that contain from 2 to 10 methylene groups. With the exception of DM_{C2}, the inhibitory potency of diamines increases with each additional methylene group. All the diamines blocked the channel in a voltage-dependent manner. The voltage dependence of channel block by various diamines is more clearly shown in Fig. 4, in which we plotted the fraction of unblocked current in the presence of each diamine as a function of membrane voltage. The blocking curves corresponding to various diamines are quite different. Those for DM_{C2}, DM_{C3}, DM_{C6}, and DM_{C7} have mainly two phases: a descending phase followed by an ascending phase. As discussed earlier, the curve for
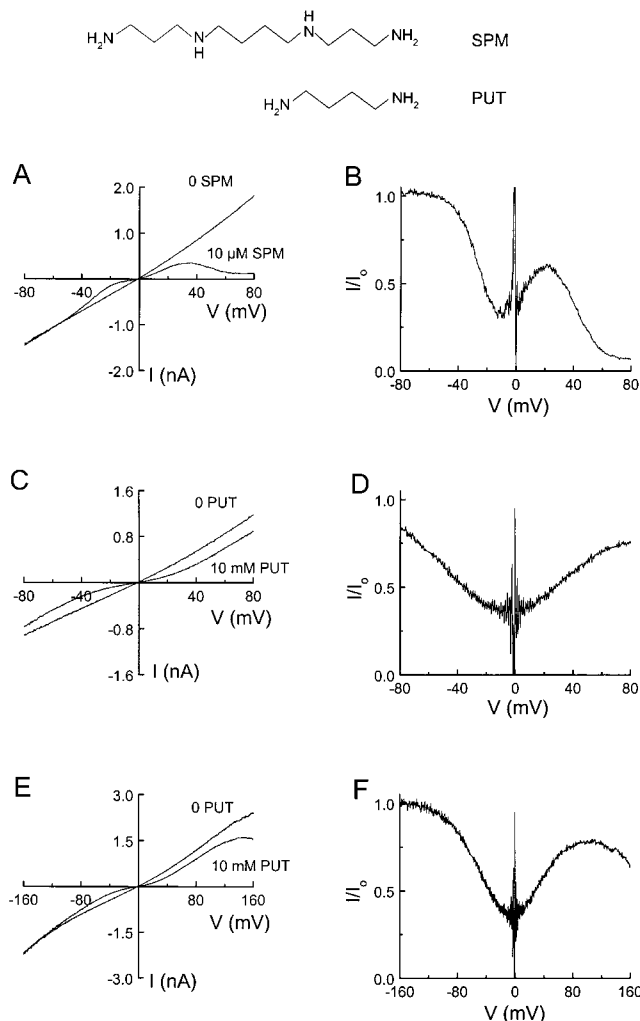
785   Guo and Lu

Figure 2. Comparison of CNG channel block by intracellular spermine and putrescine. (A) I-V curves of the CNG channel in the absence and presence of 10 μM spermine (SPM). (B) The fraction of current not blocked by 10 μM spermine is plotted against membrane voltage. (C and E) I-V curves of the channel in the absence and presence of 10 mM of putrescine (PUT), over different voltage ranges. (D and F) The fractions of current not blocked by 10 mM putrescine, obtained from C and E, are plotted against membrane voltage.

DM_{C4} (putrescine) has a very prominent second descending phase, and consequently shows a minimum followed by a maximum. Interestingly, for DM_{C5}, the minimum and maximum seem to merge into an extended plateau that precedes a second descending phase. The curves corresponding to DM_{C8} through DM_{C10} simply approach a nonzero level at the end of the experimentally accessible voltage range.

Block of the CNG Channel by Spermine at Two Different Intracellular pH

To gain insight into the effect of polyamine charge on channel block, we altered the average number of charged amines in spermine by adjusting intracellular pH, exploiting the fact that the pKa for some amine groups is in the range of 8 to 9 (Palmer and Powell, 1974). Fig. 5 A shows the I-V curves of the CNG channel without and with 10 μM spermine at intracellular pH 7.6 or 8.6. Altering intracellular pH had little effect on the control I-V curve. However, it dramatically affected channel block by spermine, which can be more clearly seen in Fig. 5 B, where the ratios of currents with and without spermine at the two intracellular pH values are plotted against membrane voltage. Raising intracellular pH shifts the first descending phase to slightly more positive membrane voltages, but more dramatically shifts the second descending phase to less positive voltages. Increasing intracellular pH also reduces the amplitude of the intervening ascending phase. However, the slopes of both blocking phases appear to be little affected by intracellular pH.

Block of the CNG Channel by Spermine and Spermidine Over a Wider Voltage Range

Fig. 6, A and B, shows the I-V curves of the CNG channel in the absence or presence of spermine and spermidine, while C and D shows the fractions of current not blocked by spermine and spermidine, respectively, against membrane voltage. Over this much wider range of membrane voltage (−180 to +180 mV), the curve for spermine now displays two pairs of minima and maxima. Although the multiple phases in the curves for spermidine are not as well defined (Fig. 6 D), the curve for 100 μM spermidine has a small "minimum" (indicated by an arrow) at voltages where the second minimum in the spermine curve occurs (compare C with D). We have repeated this measurement many times and the small "minimum" in the 100 μM spermidine curve was invariably observed. Thus, the blocking curves for spermidine and spermine are likely fundamentally similar—two pairs of minima and maxima at comparable membrane voltages—although the multiple phases are poorly separated in the case of spermidine.

Block of the CNG Channel by Spermine at Various Concentrations of cGMP

To test whether block of the CNG channel by polyamines depends on cGMP concentration, we examined channel block by spermine at various concentrations of cGMP. Fig. 7, A–F, shows the I-V curves for the channel in the absence and presence of various concentrations of spermine, as the concentration of cGMP was varied from 10 μM to 1 mM ($K_{1/2}$ for cGMP is ~80 μM). In the presence of spermine, the shape of the I-V curves at positive membrane voltages varied significantly with the concentration of cGMP. The variations are more clearly shown in Fig. 7, G–L, which shows the fractions of unblocked current as a function of membrane volt-
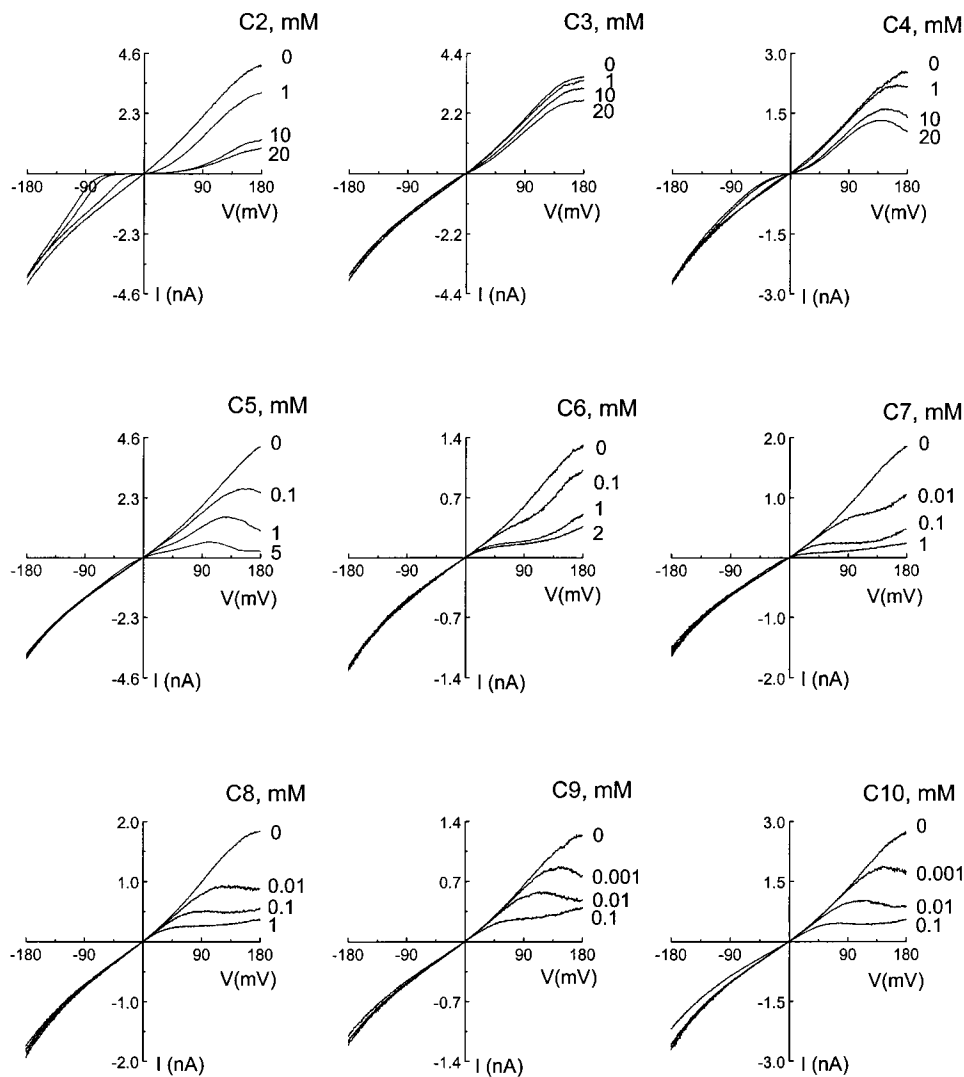
Figure 3. Effect of diamines on the current–voltage relationship of the CNG channel. I-V curves were obtained in the absence and presence of nine diamines (DM_{C2} through DM_{C10}, labeled as C_2 through C_{10}) at the various concentrations indicated.

age. The first descending and ascending phases are very similar at all cGMP concentrations tested. The second descending phase became steeper, and a second ascending phase became apparent, when the cGMP concentration was increased to 30 μM. The third descending phase did not appear until cGMP was increased to 50 μM. In other words, the first minimum and maximum pair was present at all concentrations of cGMP, but the second minimum and maximum pair at positive voltages, absent at 10 μM cGMP, gradually appeared when cGMP concentration was raised.

Block of the CNG Channel by a Spermine Derivative

To test whether depolarization-induced relief of channel block results from spermine permeation, we studied the blocking behavior of a natural derivative of spermine isolated from a spider venom, called PhTx. PhTx can be thought of as spermine with a bulky group attached to one end. Fig. 8 A shows the I-V curves of the channel in the absence and presence of PhTx at the concentrations indicated. Unlike the complex I-V curves obtained in the presence of spermine (see Fig. 6 A), the I-V curves in the presence of PhTx merely display a downward curvature, as expected for a nonpermeant ionic pore blocker. Fig. 8 B shows that the fraction of unblocked current in the presence of PhTx decreases with increasing membrane voltage. No significant voltage-induced relief of channel block by PhTx was observed between −180 to +180 mV.

DISCUSSION

The extent of CNG channel block by intracellular polyamines varies with membrane voltage in a complex manner. For example, when membrane voltage is increased from −80 to +80 mV in the presence of spermine, the CNG current varies in three phases: two descending phases with an intervening ascending phase, resulting in a minimum followed by a maximum in the voltage-dependent blocking curve (Fig. 2 B). A similar
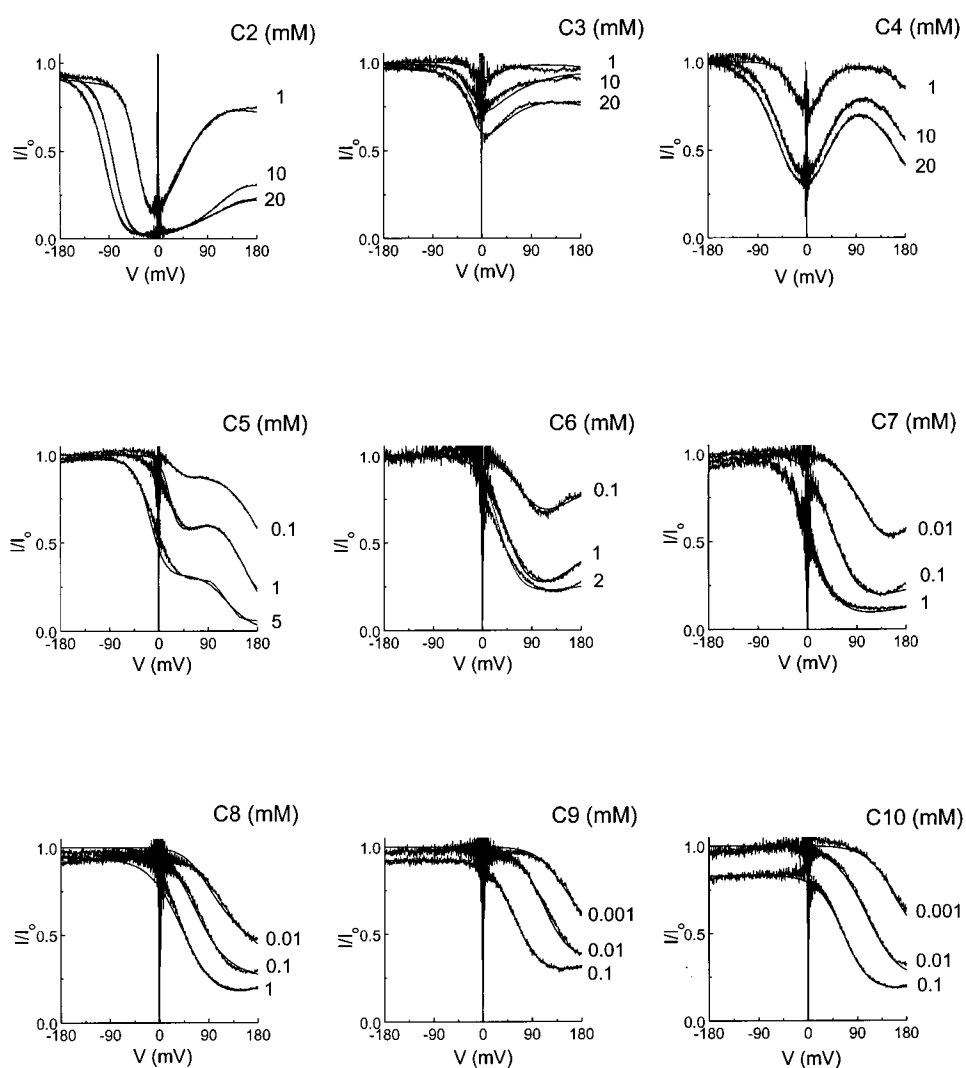
Figure 4. Voltage dependence of CNG channel block by various diamines. The fraction of current not blocked by nine diamines (DM_{C2} through DM_{C10}, labeled as C_2 through C_{10}) at various concentrations is plotted against membrane voltage. The curves superimposed on the data are fits of Eqs. 5 or 6 (see discussion).

phenomenon, although occurring over a much wider range of membrane voltage, was also observed with polyamines containing fewer amine groups; e.g., putrescine (Fig. 2 F). As proposed previously, the first and second descending phases in the relative current versus membrane voltage plot can be attributed to channel block by a polyamine molecule in one of two conformations with different affinity, while the intervening ascending phase can be accounted for by permeation of the polyamine in its higher affinity conformation and consequent resumption of ionic current (Lu and Ding, 1999). The interesting and complex blocking behavior observed here can occur only when channel block by the more permeant conformation occurs at much lower membrane voltages.

To test whether the depolarization-induced relief of channel block results from polyamine permeation, we examined channel block by PhTx, a derivative of spermine whose one end is attached to a bulky chemical group. Such a chemical modification was previously

shown to dramatically hinder spermine permeation through glutamate-gated channels (Bähring et al., 1997). Here, we found that depolarization up to +180 mV does not significantly relieve block of the CNG channel by PhTx (Fig. 8 B). Thus, the bulky group attached to spermine in PhTx prevents the molecule from traversing the CNG channel. Quantitatively, the voltage-dependent blocking behavior of PhTx can be accounted for by the Woodhull mechanism, arguing that PhTx acts on the CNG channel as a nonpermeant ionic pore blocker. These findings support the idea that the depolarization-induced relief of polyamine block in the CNG channel results from polyamine permeation and subsequent resumption of Na^+ ion passage.

Analysis of Channel Block by Various Diamines

To gain insight into the complex blocking behaviors of diamines with methylene chains of varying length, we analyzed the blocking curves of the various diamines
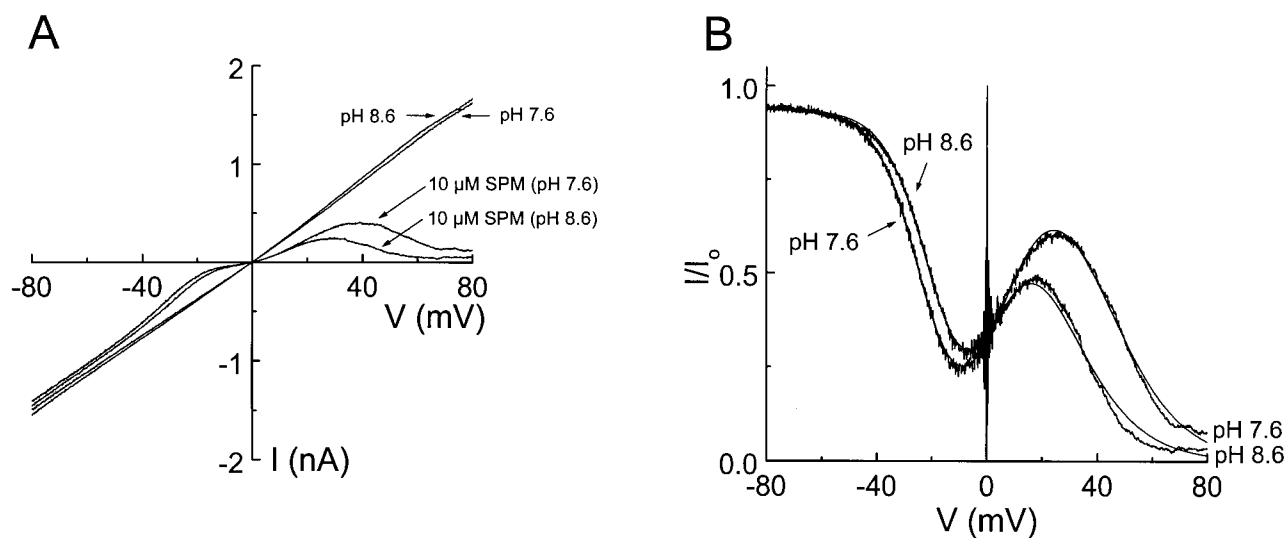
Figure 5. Intracellular pH dependence of CNG channel block by intracellular spermine. (A) I-V curves of the CNG channel in the absence and presence of 10 μM spermine at intracellular pH 7.6 and 8.6. Extracellular pH was 7.6 in both cases. (B) Ratios of the I-V curves at the corresponding pH, shown in A, are plotted against membrane voltage. The smooth curves were obtained by simultaneous fitting of the two data curves using Eq. 7. The values of all parameters obtained from fitting are: $K_1^a = 0.51 \pm 0.04$ μM, $Z_1^a = 3.0 \pm 0.1$, $k_{-2}^a / k_{-1}^a = 8.5 \pm 0.3$, "$z_{-2}^a + z_{-1}^a$" $= 5.5 \pm 0.1$, $K_1^b = 45.9 \pm 0.9$ μM; $Z_{-1}^b = 1.8 \pm 0.1$, and pKa $= 9.1 \pm 0.1$ (mean $\pm$ SEM, $n = 3$).
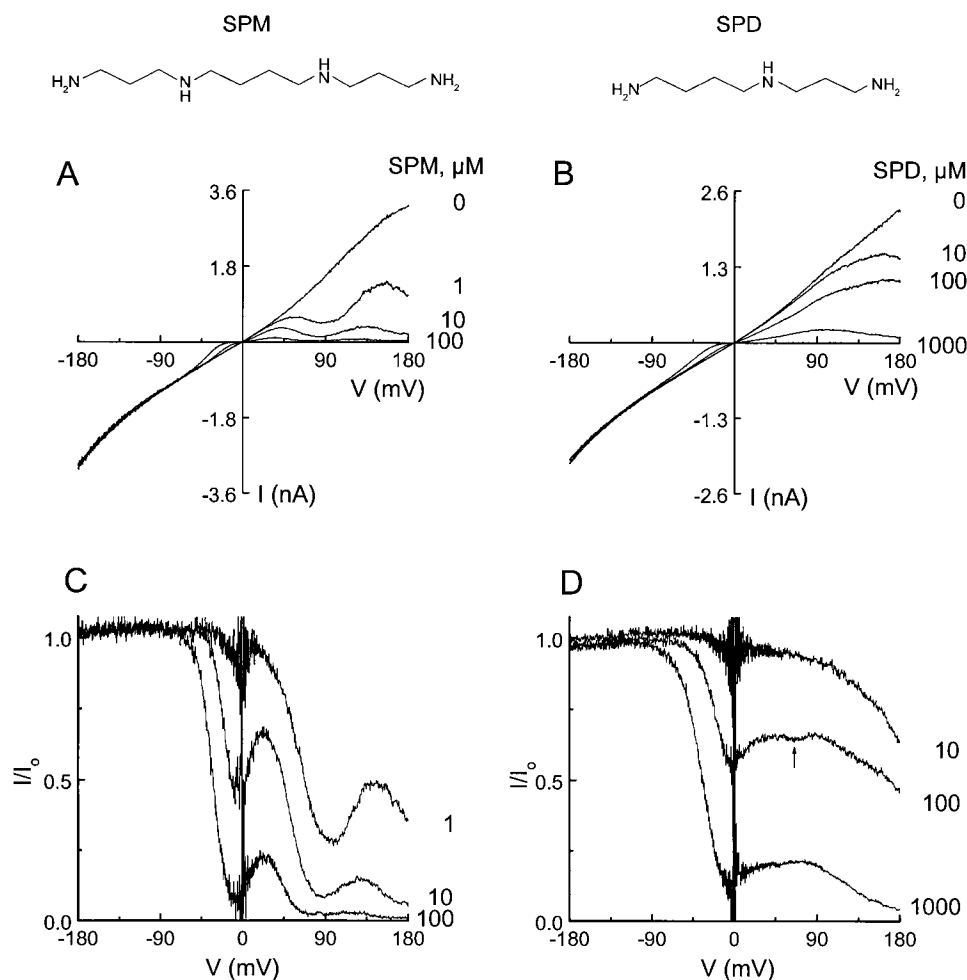

Figure 6. Block of the CNG channel by intracellular spermine and spermidine over a wider voltage range. (A and B) I-V curves of the CNG channel without or with spermine and spermidine, respectively, at the concentrations indicated. (C and D) The fractions of current not blocked by spermine and spermidine, respectively, are plotted against membrane voltage.
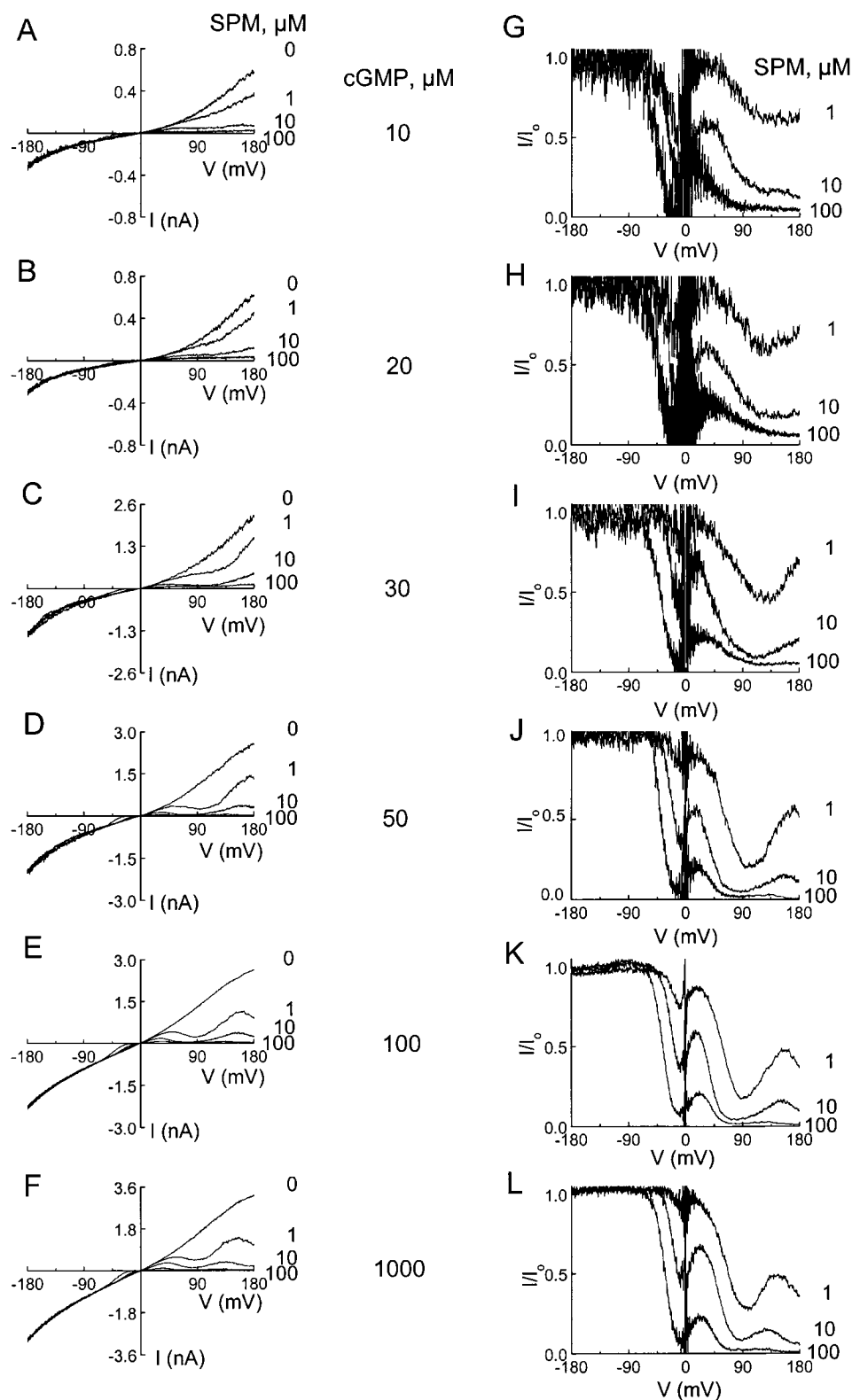
789   Guo and Lu

Figure 7. Cyclic GMP concentration dependence of CNG channel block by spermine. (A–F) I-V curves of the channel without and with spermine at various cGMP concentrations. (G–L) The fractions of current not blocked by spermine at various spermine and cGMP concentrations are plotted against membrane voltage.

using a model shown in Fig. 9 A, similar to one previously used to analyze spermine block of this channel (Lu and Ding, 1999). The model assumes that a diamine (*DM*) blocks the channel in one of two (slightly)

permeant conformations, *a* and *b*, resulting in two blocked states. Interconvertibility between the two blocked states cannot be assessed based on the steady state data presented here. For simplicity, our model as-
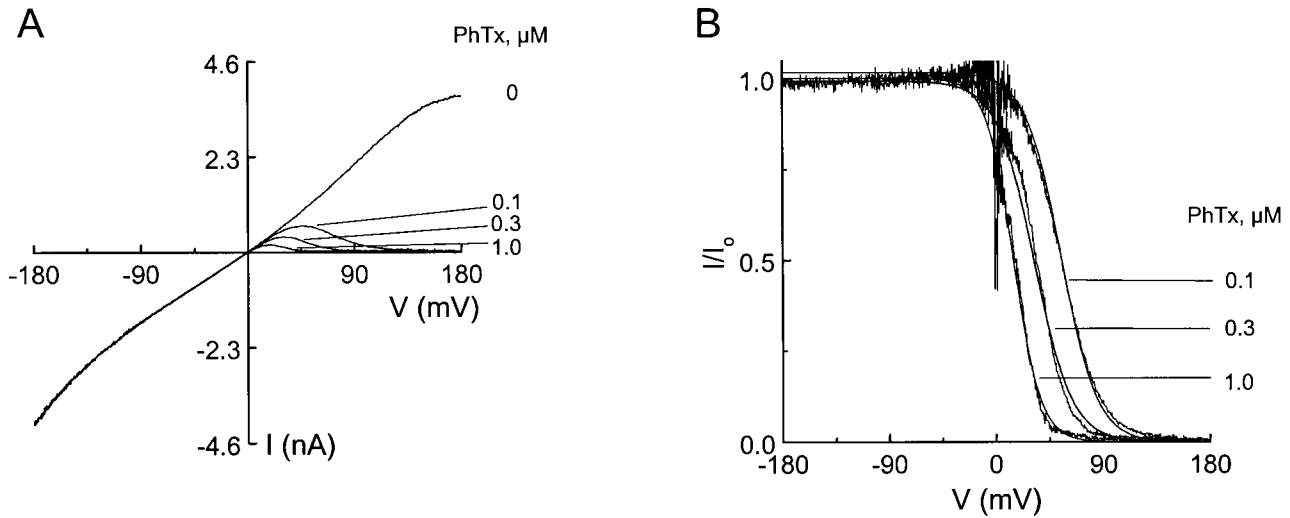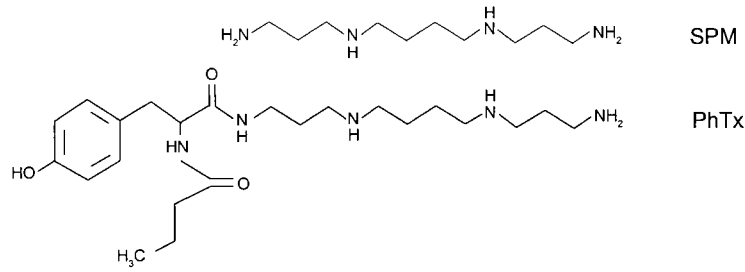
Figure 8. Block of the CNG channel by a spermine derivative. (A) I-V curves without or with three concentrations of a spermine derivative, PhTx. (B) The fractions of current not blocked by PhTx are plotted against membrane voltage. The curves superimposed on the data are fits of the Woodhull equation, $I/I_o = 1/(1 + [\text{PhTx}]/K_d e^{-ZFV/RT}$. The K_d and Z determined from the fits are 2.8 ± 0.5 μM and 1.8 ± 0.3 (mean $\pm$ SEM, $n = 4$).

sumes no direct transition between the two blocked states. The fraction of unblocked channels, and thus that of unblocked current, is then given by Eq. 1:

$$\frac{I}{I_o} = \frac{[Ch]}{[Ch] + [Ch \cdot DM^a] + [Ch \cdot DM^b]}. \tag{1}$$

Using rate constants, we obtain:

$$\frac{I}{I_o} = \frac{1}{1 + [DM]\left(\dfrac{k_1^a}{k_{-1}^a + k_{-2}^a} + \dfrac{k_1^b}{k_{-1}^b + k_{-2}^b}\right)}, \tag{2}$$

where $[DM]$ is the intracellular diamine concentration (the extracellular diamine concentration is zero). Assuming the second conformation is nonpermeant (i.e., $k_{-2}^b = 0$), Eq. 2 becomes:

$$\frac{I}{I_o} = \frac{1}{1 + [DM]\left(\dfrac{k_1^a}{k_{-1}^a + k_{-2}^a} + \dfrac{1}{K_1^b}\right)}, \tag{3}$$

where $K_1^b = k_{-1}^b / k_1^b$, the equilibrium dissociation constant for the nonpermeant form. Further assuming that
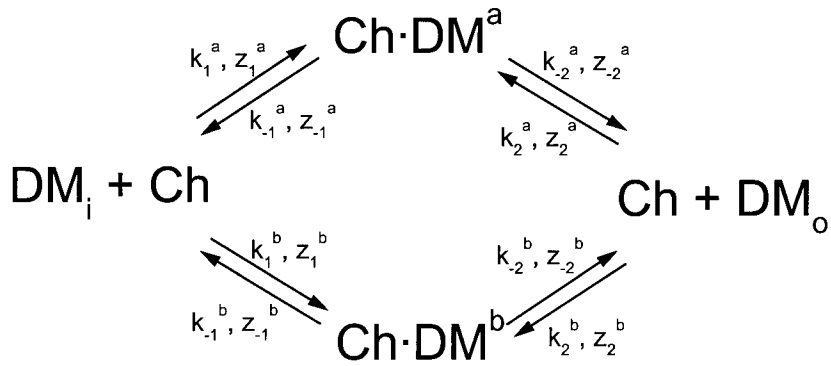
all rate constants vary exponentially with membrane voltage, Eq. 3 becomes:

$$\frac{I}{I_o} = \frac{1}{1 + [DM]\left[\dfrac{k_1^a e^{\frac{z_1^a FV_m}{RT}}}{k_{-1}^a e^{\frac{-z_{-1}^a FV_m}{RT}} + k_{-2}^a e^{\frac{z_{-2}^b FV_m}{RT}}} + \dfrac{1}{K_1^b e^{\frac{-Z_1^b FV_m}{RT}}}\right]} \tag{4}$$
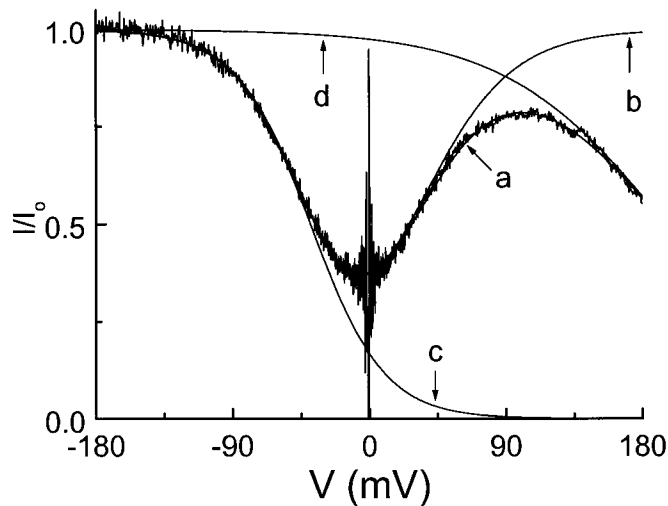
or

$$\frac{I}{I_o} = \tag{5}$$

$$\frac{1}{1 + [DM]\left[\dfrac{1}{\left(1 + \dfrac{k_{-2}^a}{k_{-1}^a} e^{\frac{(z_{-1}^a + z_{-2}^a)FV_m}{RT}}\right) K_1^a e^{\frac{-Z_1^a FV_m}{RT}}} + \dfrac{1}{K_1^b e^{\frac{-Z_1^b FV_m}{RT}}}\right]}$$

791   Guo and Lu

A

B

Figure 9. A kinetic model for CNG channel block by diamines. (A) Reaction scheme. Ch represents the CNG channel, DM_i and DM_o denote intra- and extracellular diamines, and $Ch \cdot DM^a$ and $Ch \cdot DM^b$ denote the CNG channels blocked by DM in two conformations, respectively. Rate constants at 0 mV (k_x or k_{-x}) and the corresponding valence number (z_x or z_{-x}) are indicated. (B) Noisy experimental trace plots the fraction of current not blocked by 10 mM putrescine against membrane voltage. Curve a superimposed on the data is a fit of Eq. 5. The fit gives $K_1^a = 2.0$ mM, $Z_1^a = 1.1$, $k_{-2}^a/k_{-1}^a = 2.0$, "$z_{-2}^a + z_{-1}^a$" = 1.9, $K_1^b = 388.2$ mM, and $Z_{-1}^b = 0.5$. The other three curves correspond to three hypothetical cases using the corresponding parameters from the fit, except that putrescine is assumed to act (b) as a pure high-affinity permeant blocker ($K_1^b = \infty$), (c) as a pure high-affinity non-permeant blocker ($K_1^b = \infty$ and $k_{-2}^a = 0$), or (d) as a low affinity nonpermeant blocker for curve d ($K_1^a = \infty$ and $k_{-2}^b = 0$).

where $K_1^a = k_{-1}^a/k_1^a$ is the equilibrium dissociation constant for the permeant form, and quantities z_i^x and Z_i^x are the apparent valences associated with the corresponding constants. V_m is membrane voltage, and F, R, and T have their usual meanings.

Fig. 9 B illustrates how the various transitions in the model (or the various constants in Eqs. 4 or 5) are related to the different phases in a putrescine (DM_{C4})-blocking curve. Curve a superimposed on the data is a fit of Eq. 5, while the other three curves correspond to three hypothetical cases: putrescine acting as (b) a single-conformation, high-affinity, permeant blocker ($K_1^b = \infty$), (c) a single-conformation, high-affinity, nonpermeant blocker ($K_1^b = \infty$ and $k_{-2}^a = 0$), or (d) a single-conformation, low-affinity, nonpermeant blocker ($K_1^a = \infty$ and $k_{-2}^b = 0$). The values of the corresponding parameters used to generate curves b–d are the same as those for the full curve a. Thus, the first and second descending phases of the blocking curve are accounted for by channel block by putrescine in the high- and low-affinity conformations, respectively, while the intervening ascending phase reflects permeation of putrescine in the high-affinity conformation. Since k_{-2}^a/k_{-1}^a is the relative

probability of a diamine bound in the pore escaping to the external solution versus returning to the intracellular solution, it provides a measure of diamine permeation. Quantities k_{-2}^a/k_{-1}^a and "$z_{-1}^a + z_{-2}^a$" were treated as single adjustable parameters in the fit of Eq. 5.

To analyze those blocking curves that do not display a significant second descending phase, we omitted the term K_1^b:

$$\frac{I}{I_o} = \frac{1}{1 + \left[\dfrac{[DM]}{\left(1 + \dfrac{k_{-2}^a}{k_{-1}^a} e^{\frac{(z_{-1}^a + z_{-2}^a)FV_m}{RT}}\right) K_1^a e^{\frac{-Z_1^a FV_m}{RT}}} \right]}. \quad (6)$$

Examples of analyses of diamine data using Eqs. 5 and 6 are shown in Fig 4; the curves superimposed on the data are all in fact fits of these equations. The parameters obtained from these fits are summarized in Fig. 10.

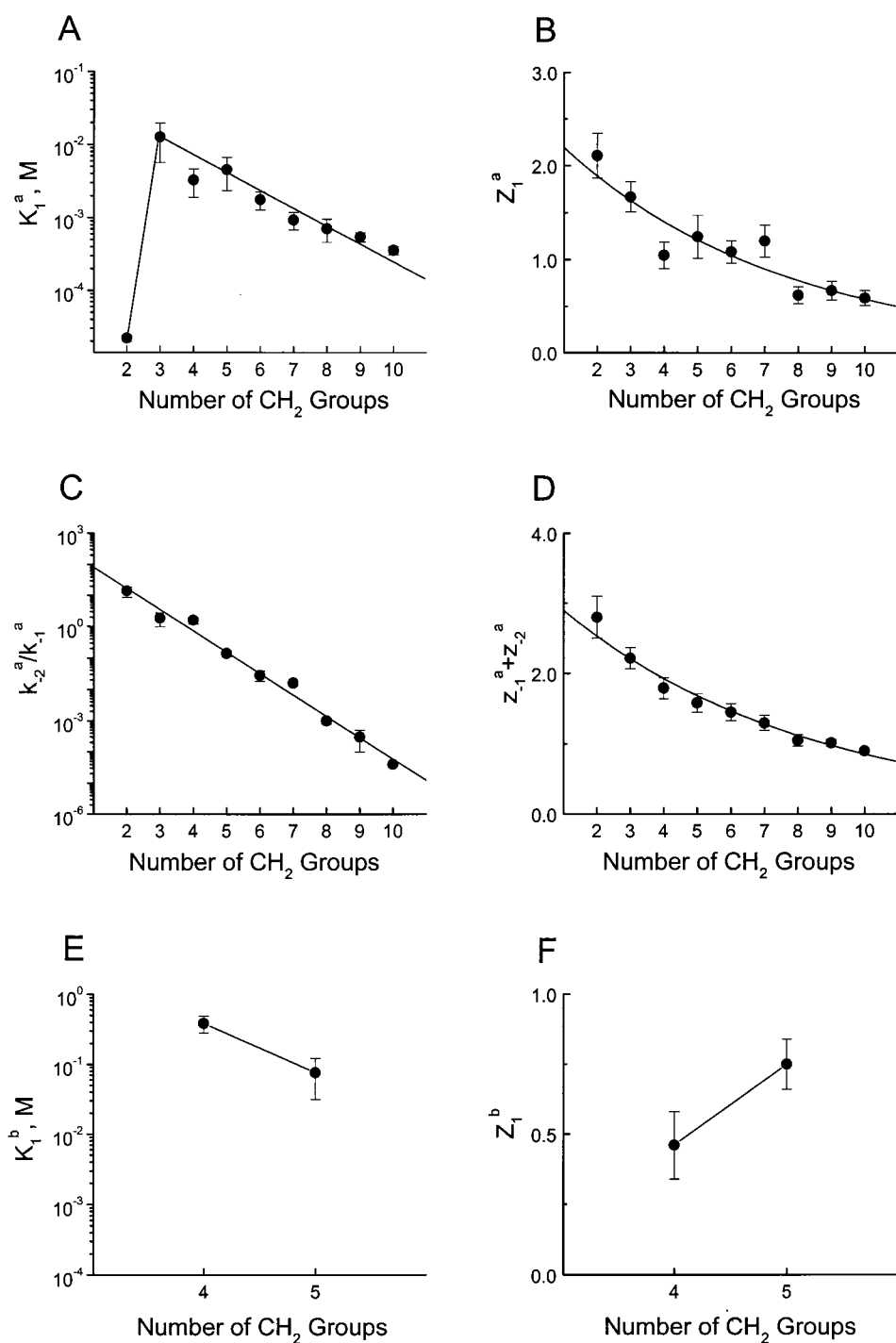Fig. 10, A and B, plot K_1^a and Z_1^a versus the number

Figure 10. Summary of the fitting parameters obtained from analyzing the diamine-blocking curves. As illustrated in Fig. 4, all diamine-blocking curves were fitted with either Eq. 5 or 6, depending on whether the fitted curve contains a second descending phase. The six adjustable parameters, plotted in A–F against number of methylene groups in the diamine chain, were $K_1{}^a$, $Z_1{}^a$, $k_{-2}{}^a/k_{-1}{}^a$, and "$z_{-2}{}^a + z_{-1}{}^a$" needed in both equations, and $K_1{}^b$ and $Z_1{}^b$ needed in Eq. 5 only. All parameters, obtained from the fits, are presented as mean ± SEM (n = 6–10).

of methylene groups in the tested diamines, respectively. These two parameters are mainly related to the first descending phase; i.e., binding and unbinding of diamines in the permeating conformation. With the exception of DM$_{C2}$, longer diamines generally have a lower $K_1{}^a$ (higher affinity), consistent with the observation that longer diamines have higher blocking potency (Fig. 3). Although the amine groups of shorter

diamines may both be located inside the narrow region, with increasing methylene chain length the trailing amine group should gradually extend out of the pore into the intracellular solution, as originally proposed for sarcoplasmic reticulum K$^+$ channel block by bis-Q compounds (di-quaternary ammoniums) (Miller, 1982). This picture can also be invoked to explain the decrease in apparent valence $Z_1{}^a$.

When the number of methylene groups in diamines increases, k_{-2}^a/k_{-1}^a becomes smaller (Fig. 10 C). Longer diamines being less likely to go across the pore to the extracellular side is consistent with the expectation that energy barriers are higher for the longer and more hydrophobic diamines. Since "$z_{-1}^a + z_{-2}^a$" decreases with diamine length, the enhancement of permeation by membrane depolarization decreases with diamine length (Fig. 10 D). These two factors together account for the observed reduction in permeation for longer diamines.

The blocking curves of both DM_{C4} and DM_{C5} have a rather prominent second blocking phase, a behavior apparently associated with methylene chain length between the amine groups. Thus, we used the full Eq. 5 to analyze their behavior. We found that the K_1^b value of DM_{C5} is significantly lower (high affinity) than that of DM_{C4} (Fig. 10 E), whereas the apparent affinity (or K_1^a) of the high-affinity conformations of the two diamines is comparable (Fig. 10 A). These findings are compatible with the observation that the first and second blocking phases of DM_{C5} are less well separated. The reduced separation of the two blocking phases and the lower permeability (k_{-2}^a/k_{-1}^a) of DM_{C5} together explain why the minimum and maximum that clearly separate the two blocking phases in the case of DM_{C4} become merged into an extended plateau in the case of DM_{C5} (Fig. 4).

Although various diamines exhibit rather different blocking behaviors, we found that increasing methylene chain length generally favors diamine binding, but reduces the likelihood of permeation. Thus, not surprisingly, hydrophobic forces play a critical role in the interactions between channel and diamines.

Protonation Underlies the Different Blocking Conformations of Polyamines

Ammonia has a pKa value of 9.3. Attaching an alkyl group of arbitrary length to the nitrogen atom raises its pKa to a nearly uniform value around 10.6 (Albert and Serjeant, 1971). For example, pKa values for the monoamines methylamine (C_1), octylamine (C_8), and docosylamine (C_{22}) are 10.66, 10.65, and 10.60, respectively. When a second alkyl group is added to form a secondary amine, the additional pKa perturbation is much smaller. In the case of diamines, protonation of the first amine group significantly affects protonation of the second group. As expected for an electrostatic effect, this pK perturbation in diamines diminishes as the intervening methylene chain length increases. Comparing four diamines, DM_{C2}, DM_{C3}, DM_{C4} and DM_{C8}, the pKa values for the first protonation are 10.1, 10.6, 10.8, and 11.0, while those for the second protonation are 7.0, 8.6, 9.4, and 10.1, respectively. Similar pKa perturbations occur in spermine. Palmer and Powell (1974)

determined four distinct pKa values for spermine (10.8, 10.0, 8.9, and 8.0 at 100 mM ionic strength and 25°C). Although the exact assignment of pKa values in spermine is uncertain, the finding implies that a significant fraction of spermine molecules is not fully protonated at pH 7.6, where we examined CNG channel block by spermine.

We surmise that the hypothesized multiple blocking conformations of spermine represent its different protonated states, the more protonated species corresponding to the higher-affinity, more permeant conformation, and the less protonated species corresponding to the lower-affinity, less permeant conformation. If this is true, altering intracellular pH should alter the spermine-blocking curve in the following manner. At a given spermine concentration, raising intracellular pH deprotonates spermine and thus decreases its fraction in the high-affinity form, which should shift the first blocking (descending) phase to more positive membrane voltages. Simultaneously, the increased fraction in the low-affinity (less protonated) form should shift the second blocking (descending) phase to lower voltages. As the two blocking phases are now closer to one another, the amplitude of the intervening ascending phase (reflecting permeation of the high-affinity form) should decrease. The steepness (apparent voltage dependence) of the two blocking phases should be unaffected by pH, because each reflects how the channels interact with a given form of spermine, not its concentration. This is, indeed, what we observed when we raised intracellular pH from 7.6 to 8.6. Fig. 5 B plots the fraction of unblocked current in the presence of 10 µM spermine at intracellular pH 7.6 and 8.6. We analyzed the data according to the scheme shown in Fig. 11, which assumes that the two spermine conformations reflect the titration of a single amine group. The fraction of unblocked current in the presence of spermine is then given by:

$$\frac{I}{I_o} = \tag{7}$$

$$\frac{1}{1 + [PM]\left[\dfrac{\theta}{\left(1 + \dfrac{k_{-2}^a}{k_{-1}^a}e^{\frac{(z_{-1}^a + z_{-2}^a)FV_m}{RT}}\right)K_1^a e^{\frac{-Z_1^a FV_m}{RT}}} + \dfrac{1 - \theta}{K_1^b e^{\frac{-Z_1^b FV_m}{RT}}}\right]}$$

where $\Theta = 10^{-pH}/(10^{-pH} + 10^{-pKa})$. The two smooth curves superimposed on the blocking curves obtained at intracellular pH 7.6 and 8.6 are simultaneous fits of Eq. 7; i.e., all the fitting parameters are the same for both curves. The pKa of the titrated amine group, de-
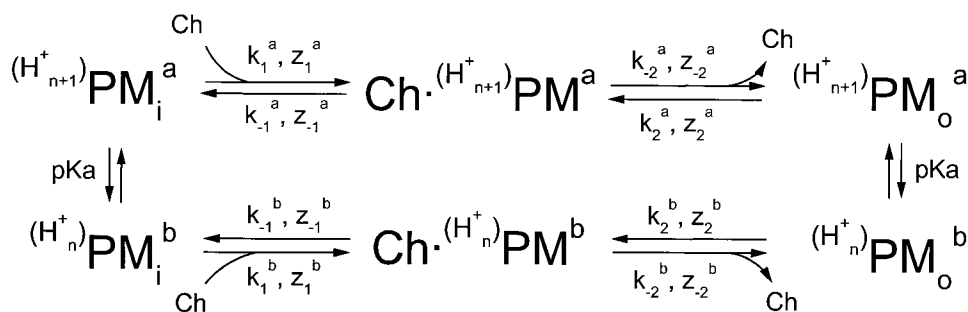
$(H^+_{n+1})PM_i^a \xrightleftharpoons[k_{-1}^a, z_{-1}^a]{k_1^a, z_1^a} \;Ch \cdot {}^{(H^+_{n+1})}PM^a \xrightleftharpoons[k_2^a, z_2^a]{k_{-2}^a, z_{-2}^a}\; (H^+_{n+1})PM_o^a$

$pKa \updownarrow \qquad\qquad\qquad\qquad\qquad\qquad\qquad\qquad\qquad\qquad \updownarrow pKa$

$(H^+_n)PM_i^b \xrightleftharpoons[k_1^b, z_1^b]{k_{-1}^b, z_{-1}^b} \;Ch \cdot {}^{(H^+_n)}PM^b \xrightleftharpoons[k_{-2}^b, z_{-2}^b]{k_2^b, z_2^b}\; (H^+_n)PM_o^b$

Figure 11. A kinetic model for pH dependence of CNG channel block by polyamines. The model essentially is the same as that in Fig. 9 A, except that polyamine molecules can be in either a more or a less protonated form.

termined from the fit, is 9.1 ± 0.1 (mean ± SEM; $n = 3$), very close to 8.9, the second lowest pKa value of spermine (Palmer and Powell, 1974). Thus, the data can be accounted for by a model in which the two observed blocking conformations of spermine result from titrating the amine group with the second lowest pKa value. The model is also compatible with the finding that the values of the apparent valence associated with each of the blocking conformations are 3.0 ± 0.1 and 1.8 ± 0.1 (mean ± SEM), respectively. Thus, it is understandable why channel block by the higher-affinity (higher charge) form of spermine is more voltage dependent than that by the lower-affinity (lower-charge) form.

Although the observed multiple blocked channel states are well accounted for by nonuniform protonation of the blocking agent, they can in principle be equally well accounted for by different protonation states of the channel. In the olfactory CNG channel, protonation of a glutamate residue (equivalent to E363 in the retinal channel), located at the external end of the pore, reduces the single-channel conductance (Root and MacKinnon, 1994). Moreover, residue E363 in the retinal CNG channel forms the binding site for external divalent cations and also affects the binding of internal divalent cations to the pore (Root and MacKinnon, 1993; Eismann et al., 1994; Park and MacKinnon, 1995). To examine whether the multiple spermine-induced blocked states result from nonuniform protonation of E363, we examined spermine block of the E363G mutant channel in which E363 was replaced by a nonprotonatable glycine residue. With this E363G channel, we still observed the multiphasic spermine-blocking curve seen in the wild-type channel, except for a +40-mV shift, as if residue E363 merely affects spermine binding by an electrostatic mechanism (Fig. 1). Thus, the different blocking states do not primarily reflect nonuniform protonation of residue E363 in the channel.

Additional Blocking Components of Spermine Revealed with a Wider Range of Membrane Voltage

At positive voltages, the spermine-blocking curves in Fig. 5 B deviate somewhat from what is predicted by Eq. 7, which assumes for simplicity that spermine in the second blocking conformation is strictly nonpermeant.

To examine whether the second blocking conformation is also slightly permeant, we examined spermine block over a much wider range of membrane voltage (−180 to +180 mV). We found that, above +90 mV, channel block by spermine was significantly relieved by further depolarization (Fig. 6 C), consistent with spermine in the second blocking conformation also being permeant. Interestingly, beyond +140 mV, channel block was again enhanced. These observations argue that spermine blocks the channel in at least three conformations. Thus, to account for this extraordinary voltage dependence of channel block, a third blocking state (c) would need to be added to the model in Fig. 9 A. This third conformation (c) should bind to the channel with even less affinity and be less likely to permeate. If the first blocking conformation (a) corresponds to spermine with three (and four) charged amines and the second (b) corresponds to spermine with two charged amines, then the third (c) will correspond to spermine with a single charged amine. This proposal is compatible with the observation that voltage dependence of channel block by the first blocking conformation is stronger than the second, which is stronger than the third, as manifested by the different slopes of the three blocking phases (Fig. 6 C). As already mentioned in results, spermidine appears to behave similarly, although the multiple components are much less well separated (Fig. 6 D).

Altering cGMP concentration has different effects on each of the three blocking components of spermine (Fig. 7). Lowering cGMP concentration has little effect on the first blocking component, but diminishes the second blocking phase, whereas the third blocking phase essentially vanishes at cGMP concentrations below 30 μM. These results argue that spermine conformation a occupies open and closed channels with similar affinity, b occupies open channels with higher affinity, and c essentially occupies only open channels. Previous studies showed that decreasing cGMP concentrations enhances block of the CNG channel by intracellular tetracaine (Fodor et al., 1997). The cGMP dependence of channel block by intracellular cations most likely reflects conformational changes of the pore resulting from channel gating.

795   Guo and Lu

REFERENCES

Albert, A., and E.P. Serjeant. 1971. The determination of ionization constants (a laboratory manual). Chapman and Hall Ltd. London, UK.

Araneda, R.C., R.S. Zukin, and M.V.L. Bennett. 1993. Effects of polyamines on NMDA-induced currents in rat hippocampal neurons: a whole-cell and single channel study. *Neurosci. Lett.* 152: 107–112.

Ault, B., R.H. Evans, A.A. Francis, D.J. Oakes, and J.C. Witkins. 1980. Selective depression of excitatory amino acid induced depolarization by magnesium ions in isolated spinal cord preparations. *J. Physiol.* 307:413–428.

Bader, C.R., P.R. Macleish, and E.A. Schwartz. 1979. A voltage-clamp study of the light response in solitary rods of the tiger salamander. *J. Physiol.* 296:1–26.

Bähring, R., D. Bowie, M. Benveniste, and M.L. Mayer. 1997. Permeation and block of the rat GluR6 glutamate receptor channels by internal and external polyamines. *J. Physiol.* 502:575–589.

Bastian, B.L., and G.L. Fein. 1982. The effects of sodium replacement on the responses of toad rods. *J. Physiol.* 330:331–347.

Baylor, D.A., and B.J. Nunn. 1986. Electrical properties of the light-sensitive conductance of salamander rods. *J. Physiol.* 371:115–145.

Benveniste, M., and M.L. Mayer. 1993. Multiple effects of spermine on *N*-methyl-d-aspartic acid receptor responses of rat cultured hippocampal neurons. *J. Physiol.* 464:131–163.

Bododia, R.D., and P.B. Detwiler. 1985. Patch-clamp recordings of the light-sensitive dark noise in retinal rods from the lizard and frog. *J. Physiol.* 367:183–216.

Bowie, D., and M.L. Mayer. 1995. Inward rectification of both AMPA and kainate subtype glutamate receptors generated by polyamine-mediated ion channel block. *Neuron.* 15:453–462.

Bowie, D., G.D. Lange, and M.L. Mayer. 1998. Activity-dependent modulation of glutamate receptors by polyamines. *J. Neurosci.* 18: 8175–8185.

Capovilla, M., A. Caretta, L. Cervetto, and V. Torre. 1983. Ionic movements through light-sensitive channels of toad rods. *J. Physiol.* 343:295–310.

Chao, J., N. Seiler, J. Renault, K. Kashiwagi, T. Masuko, K. Igarashi, and K. Williams. 1997. N^1-Dansyl-spermine and N^1-(*n*-octanesulfonyl)-spermine, novel glutamate receptor antagonists: block and permeation of *N*-methyl-d-aspartate receptors. *Mol. Pharmacol.* 51:861–871.

Colamartino, G., A. Menini, and V. Torre. 1991. Blockade and permeation of divalent cations through the cyclic GMP-activated channel from tiger salamander retinal rods. *J. Physiol.* 440:189–206.

Cu, C., R. Bähring, and M.L. Mayer. 1998. The role of hydrophobic interactions in binding of polyamines to non NMDA receptor ion channels. *Neuropharmacology.* 37:1381–1391.

Donevan, S.D., and M.A. Rogawski. 1995. Intracellular polyamines mediate inward-rectification of Ca^{2+}-permeable α-amino-3-hydroxy-

5-methyl-4-isoxazoleproprionic acid receptors. *Proc. Natl. Acad. Sci. USA.* 92:9298–9302.

Eismann, E., F. Muller, S.H. Heinemann, and U.B. Kaupp. 1994. A single negative charge within the pore controls rectification, Ca^{2+} blockage, and ion selectivity. *Proc. Natl. Acad. Sci. USA.* 91: 1109–1113.

Fakler, B., U. Brandle, E. Glowatzki, S. Weidemann, H.P. Zenner, and J.P. Ruppersburg. 1995. Strong voltage-dependent inward-rectification of inward-rectifier K^+ channels is caused by intracellular spermine. *Cell.* 80:149–154.

Ficker, E., M. Taglialatela, B.A. Wible, C.M. Henley, and A.M. Brown. 1994. Spermine and spermidine as gating molecules for inward rectifier K^+ channels. *Science.* 266:1068–1072.

Fodor, A.A., S.E. Gordon, and W.N. Zagotta. 1997. Mechanism of tetracaine block of cyclic nucleotide-gated channels. *J. Gen. Physiol.* 109:3–14.

Goulding, E.H., J. Ngai, R.H. Kramer, S. Colicos, R. Axel, S.A. Siegelbaum, and A. Chess. 1992. Molecular cloning and single channel properties of the cyclic nucleotide–gated channel from catfish olfactory neurons. *Neuron.* 8:45–58.

Goulding, E.H., G.R. Tibbs, D. Liu, and S.A. Siegelbaum. 1993. Role of H5 domain in determining pore diameter and ion permeation through cyclic nucleotide–gated channels. *Nature.* 364: 61–64.

Goulding, E.H, G.R. Tibbs, and S.A. Siegelbaum. 1994. Molecular mechanisms of cyclic-nucleotide–gated channel activation. *Nature.* 327:369–374.

Guo, D., and Z. Lu. 2000. Mechanism of IRK1 channel block by intracellular polyamines. *J. Gen. Physiol.* 115:799–813.

Haghighi, A.P., and E. Cooper. 1998. Neuronal nicotinic acetylcholine receptors are blocked by intracellular spermine in a voltage-dependent manner. *J. Neurosci.* 18:4050–4062.

Haynes, L.W., A.R. Kay, and K.-W. Yau. 1986. Single cyclic GMP-activated channel activity in excised patches of rod outer segment membrane. *Nature.* 321:66–70.

Hodgkin, A.L., P.A. McNaughton, B.J. Nunn, and K.-W. Yau. 1984. Effects of ions on retinal rods from *Bufo marinus*. *J. Physiol.* 350: 649–680.

Hodgkin, A.L., P.A. McNaughton, and B.J. Nunn. 1985. The ion selectivity and calcium dependence of the light-sensitive pathway in toad rods. *J. Physiol.* 358:447–468.

Horie, M., H. Irisawa, and A. Noma. 1987. Voltage-dependent magnesium block of adenosine-triphosphate-sensitive potassium channel in guinea-pig ventricular cells. *J. Physiol.* 387:251–272.

Ifune, C.K., and J.H. Steinback. 1991. Voltage-dependent block by magnesium of neuronal nicotinic acetylcholine receptor channel in rat phaeochromocytoma cells. *J. Physiol.* 443:683–701.

Igarashi, K., and K. Williams. 1995. Antagonist properties of polyamines and bis(ethyl)polyamines at *N*-methyl-d-aspartate receptors. *J. Pharmacol. Exp. Ther.* 272:1101–1109.

Isa, T., M. Iino, S. Itazawa, and S. Ozawa. 1995. Spermine mediates inward-rectification of Ca^{2+} permeable AMPA receptor channels. *Neuroreport.* 6:2045–2048.

Kamboj, S.K., G.T. Swanson, and S.G. Cull-Candy. 1995. Intracellular spermine confers rectification on rat calcium permeable AMPA and kainate receptors. *J. Physiol.* 486:297–303.

Kaupp, U.B., T. Niidome, T. Tanabe, S. Terada, W. Baningk, W. Stühmer, N. Cook, K. Kangawa, H. Matsuo, T. Hirose, and S. Numa. 1989. Primary structure and functional expression from complementary DNA of rod photoreceptor cyclic GMP-gated channel. *Nature.* 342:283–292.

Koh, D.S., N. Burnashey, and P. Jonas. 1995. Block of native Ca^{2+}-permeable AMPA receptors in rat brain by intracellular polyamines generates double rectification. *J. Physiol.* 486:305–312.

Liman, E.R., J. Tytgat, and P. Hess. 1992. Subunit stoichiometry of a mammalian K^+ channel determined by construction of multimeric cDNAs. *Neuron.* 9:861–871.

Lopatin, A.N., E.N. Makhaaina, and C.G. Nichols. 1994. Potassium channel block by cytoplasmic polyamines as the mechanism of intrinsic rectification. *Nature.* 372:366–369.

Lu, Z., and L. Ding. 1999. Blockade of a retinal cGMP-gated channel by polyamines. *J. Gen. Physiol.* 113:35–43.

Mathie, A., D. Colquhoun, and S.G. Cull-Candy. 1990. Rectification of currents activated by nicotinic receptors in rat sympathetic ganglion neurons. *J. Physiol.* 427:625–655.

Matsuda, H., A. Saigusa, and H. Irisawa. 1987. Ohmic conductance through the inward-rectifier K^+ channel and blocking by internal Mg^{2+}. *Nature.* 325:156–159.

Mayer, M.L., G.L. Westbrook, and P.B. Guthrie. 1984. Voltage-dependent block by Mg^{2+} of NMDA responses in spinal cord neurons. *Nature.* 309:261–263.

Miller, C. 1982. Bis-quaternary ammonium blockers as structural probes of the sarcoplasmic reticulum K^+ channel. *J. Gen. Physiol.* 79:869–891.

Nakatani, K., and K.-W. Yau. 1988. Calcium and magnesium fluxes across the plasma membrane of the toad rod outer segment. *J. Physiol.* 395:695–729.

Nowak, L., P. Bregestovski, P. Ascher, A. Herbet, and A. Prochiantz. 1984. Magnesium gates glutamate-activated channels in mouse central neurons. *Nature.* 307:462–465.

Palmer, B.B., and H.K.J. Powell. 1974. Complex formation between 4,9-diazododecane-1, 12-diamine (spermine) and copper(II) ions and protons in aqueous solution. *J. Chem. Soc. Dalton Trans.* 19:2086–2089.

Park, C.-S., and R. MacKinnon. 1995. Divalent cation selectivity in a cyclic nucleotide–gated ion channel. *Biochemistry.* 34:13326–13333.

Rock, D.M., and R.L. Macdonald. 1992a. The polyamine spermine has multiple actions on *N*-methyl-d-aspartate receptor single-channel currents in cultured cortical neurons. *Mol. Pharmacol.* 41:83–88.

Rock, D.M., and R.L. Macdonald. 1992b. Spermine and related polyamines produce a voltage-dependent reduction of *N*-methyl-d-aspartate receptor single-channel conductance. *Mol. Pharmacol.* 42:157–164.

Root, M.J., and R. MacKinnon. 1993. Identification of an external divalent cation-binding site in the pore of a cGMP-activated channel. *Neuron.* 11:459–466.

Root, M.J., and R. MacKinnon. 1994. Two identical noninteracting sites in an ion channel revealed by proton transfer. *Science.* 256:1852–1856.

Sands, S.B., and M.E. Barish. 1992. Neuronal nicotinic acetylcholine receptor currents in phaeochromocytoma (PC12) cells: dual mechanisms of rectification. *J. Physiol.* 447:467–487.

Stern, J.H., H. Knutsson, and P.R. Macleish. 1987. Divalent cations directly affect the conductance of excised patches of rod photoreceptor membrane. *Science.* 236:1674–1678.

Sunderman, E.R., and W.N. Zagotta. 1999. Sequence of events underlying the allosteric transition of rod cyclic nucleotide–gated channels. *J. Gen. Physiol.* 113:621–640.

Torre, V., H.R. Matthews, and T.D. Lamb. 1987. Ion selectivity, blockage and control of light-sensitive conductance. *Neurosci. Res. Suppl.* 6:S25–S44.

Vandenberg, C.A. 1987. Inward rectification of a potassium channel in cardiac ventricular cells depends on internal magnesium ions. *Proc. Natl. Acad. Sci. USA.* 84:2560–2564.

Varnum, M.D., K.D. Black, and W.N. Zagotta. 1995. Molecular mechanism for ligand discrimination of cyclic nucleotide–gated channel. *Neuron.* 15:619–625.

Werblin, F.S. 1975. Regeneration of hyperpolarization in rods. *J. Physiol.* 244:53–81.

Williams, K. 1997. Modulation and block of ion channels: a new biology of polyamines. *Cell. Signal.* 9:1–13.

Woodruff, M.L., G.L. Fain, and B.L. Bastian. 1982. Light-dependent ion flux into toad photoreceptors. *J. Gen. Physiol.* 80:517–536.

Yau, K.-W., and D.A. Baylor. 1989. Cyclic GMP-activated conductance of retinal photoreceptor. *Annu. Rev. Neurosci.* 12:289–327.

Yau, K.-W., P.A. McNaughton, and A.L. Hodgkin. 1981. Effects of ions on the light-sensitive current in retinal rods. *Nature.* 292:502–505.

Yau, K.-W., and K. Nakatini. 1984. Cation selectivity of light-sensitive conductance in retinal rods. *Nature.* 309:352–354.

Zimmerman, A.L., and D.A. Baylor. 1992. Cation interactions within the cyclic GMP-activated channel of retinal rods from the tiger salamander. *J. Physiol.* 449:759–783.